arXiv:1210.5601v1 [cond-mat.str-el] 20 Oct 2012

# Boundary Hamiltonians for topological models and Projected Entangled Pair States

Norbert Schuch,[1, 2] Didier Poilblanc,[3] J. Ignacio Cirac,[4] and David Pérez-García[5]
[1] *Institut für Quanteninformation, RWTH Aachen, 52056 Aachen, Germany*
[2] *Institute for Quantum Information, California Institute of Technology, MC 305-16, Pasadena CA 91125, U.S.A.*
[3] *Laboratoire de Physique Théorique, C.N.R.S. and Université de Toulouse, 31062 Toulouse, France*
[4] *Max-Planck-Institut für Quantenoptik, Hans-Kopfermann-Str. 1, D-85748 Garching, Germany*
[5] *Dpto. Analisis Matematico and IMI, Universidad Complutense de Madrid, E-28040 Madrid, Spain*

In the ground state of a gapped spin system, the physical properties of a region of the bulk are encoded in a Hamiltonian that lives on its boundary. We study the structure of such boundary Hamiltonians for topological models in the framework of Projected Entangled Pair States (PEPS). We find that the boundary Hamiltonian decomposes into two parts: A universal part which is entirely non-local but independent of microscopic details, encoding the nature of the topological phase, and a non-universal part which is local and depends on microscopic details only. A topological phase transition is reflected by a diverging interaction length of the non-universal part.

The study of strongly correlated quantum systems is of central interest in modern condensed matter physics due to the exciting properties exhibited by those systems, in particular unconventional phases with topological order. In order to identify topological order in such systems, topological entropies [1, 2] have been applied successfully. To obtain more information about the entanglement of the system than contained in the entropy, the entanglement spectrum (ES) – i.e., the spectrum of the reduced density operator of a region – has been studied, and it has been realized that for certain systems, the low-energy part of the ES resembles the spectrum of the thermal state of a one-dimensional (1D) local *boundary Hamiltonian* which can be associated to the boundary of the region studied, and which seems to be related to the edge excitations present in the model [3–6]. While this relation between bulk entanglement spectrum, boundary Hamiltonian, and edge excitations can be made rigorous in some cases [7, 8], in most cases the boundary Hamiltonian is *a posteriori* inferred from the structure of the entanglement spectrum, and a general connection between entanglement spectrum and boundary still needs to be made.

In Ref. [9], we made progress in that direction by proving a rigorous connection between entanglement spectrum and boundary using the framework of Projected Entangled Pair States (PEPS) [10], which form the appropriate description of ground states of gapped local Hamiltonians both in conventional and topological phases [11]. We found that in trivial phases (without symmetry breaking or topological order), the boundary Hamiltonian is local, while it becomes non-local at phase transitions, allowing to identify phases by looking at the locality structure of the boundary Hamiltonian. We also found that for topological models such as the toric code or quantum double models [12] which are renormalization group (RG) fixed points, the boundary Hamiltonian becomes completely non-local, coupling all spins simultaneously. However, the question remained open of how to identify topological phases away from RG fixed points from their boundary Hamiltonian, as well as how to detect phase transitions between topological and non-topological phases.

In this paper, we establish a framework for studying the boundary Hamiltonians of systems with topological order in the framework of PEPS. We find that the boundary Hamiltonian of topological models splits into two parts. The *universal part* determines the phase of the system: It couples to a topological degree of freedom at the boundary (such as the parity) and is thus completely non-local, it couples boundaries at arbitrary distance, and it depends only on the phase of the system and not on the exact point within the phase. On the other hand, the *non-univeral* part is local (generalizing what happens for trivial phases), it does depend on the point within phase, and it vanishes under RG flows. At the phase transition, the non-universal part becomes non-local, thereby destroying the topological order contained in the universal part, again allowing to detect the phase transition at the boundary.

Let us first introduce PEPS and explain how to use them to derive 1D boundary theories from 2D models. For clarity, we restrict to square lattices on a cylinder (with length $N_h$ and circumference $N_v$). A (translational invariant) PEPS $|\psi\rangle = \sum c_{i_1\ldots i_N}|i_1,\ldots,i_N\rangle$ is described by a five-index tensor $A^i_{\alpha\beta\gamma\delta}$ (Fig. 1a, with $i$ called the *physical* and $\alpha,\beta,\gamma,\delta$ the *virtual* indices), such that the coefficient $c_{i_1\ldots i_N}$ is obtained by arranging ten-

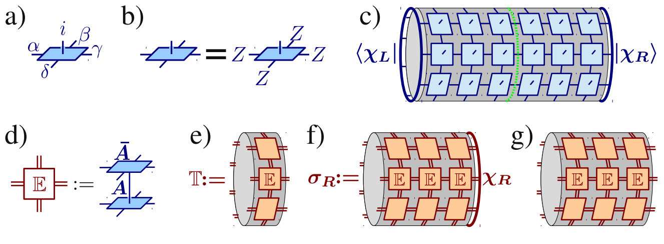

FIG. 1. Tensor networks (see text for details).

sors $A^{i_1}, \dots, A^{i_N}$ on the cylinder and contracting each virtual index with the corresponding index of the adjacent tensors, and putting some boundary conditions $|\chi_L\rangle$, $|\chi_R\rangle$ at the open virtual indices at the two ends (Fig. 1c). As proven in Ref. [9], for any PEPS the entanglement spectrum of a half-cylinder (green cut in Fig. 1c) is equal to the spectrum of $\sigma \propto \sqrt{\sigma_L^*}\sigma_R\sqrt{\sigma_L^*}$ (with $^*$ the complex conjugate), where $\sigma_R$ is the state obtained at the *virtual* indices of the right half-cylinder by contracting the physical indices with the adjoint, cf. Fig. 1d,f (with $\chi_R = |\chi_R\rangle\langle\chi_R|$, and correspondingly for $\sigma_L$). In turn, this allows to construct a *boundary Hamiltonian* $H = -\log \sigma$ which is associated to the virtual degrees of freedom at the boundary, and which exactly reproduces the entanglement spectrum. As demonstrated in [9], the phase of a system can be detected by looking at the locality of its boundary Hamiltonian: It is short-ranged in the trivial phase; the interaction length diverges at the phase transition, giving rise to a diverging correlation length; and it is long-ranged in non-trivial phases. Naturally, boundary Hamiltonians with short-range interactions are of particular interest, as they can be related to physical models. In this paper, we will reconsider the boundary Hamiltonian for non-trivial phases, and show how a local boundary Hamiltonian can be recovered.

Topological order in PEPS is accompanied by a gauge (i.e., virtual) symmetry of the tensor $A$, such as the invariance under the representation of a (finite) symmetry group, Fig. 1b [13] (more general symmetries are given, e.g., by Hopf algebras [14] or tensor categories [15]). For simplicity, we will focus on $\mathbb{Z}_2$ symmetry, i.e., $A$ is invariant under $Z^{\otimes 4}$, for some unitary representation $\{\mathbb{1}, Z\}$ of $\mathbb{Z}_2$, but our findings easily generalize to any finite group. The simplest instances of topological models are renormalization (RG) fixed points, such as the toric code [12] for $\mathbb{Z}_2$. There, the tensor $A^i$ is isometric on the symmetric subspace [13], i.e., the transfer operator $\mathbb{E}$ [Fig. 1d] equals the projector onto the symmetric subspace, $\mathbb{E} = \frac{1}{2}(\mathbb{1}^{\otimes 4} + Z^{\otimes 4})$, when understood as a map from ket to bra indices. This form of $\mathbb{E}$ is stable under contraction with itself (reflecting the fact that we are at the RG fixed point), and thus, one column of the transfer operator (Fig. 1e) equals $\mathbb{T} = \frac{1}{2}(\mathbb{1}^{\otimes 2N_v} + Z^{\otimes 2N_v})$. Again, we have that $\mathbb{T}^2 = \mathbb{T}$ as we are at the RG fixed point, and thus, the two virtual boundaries of Fig. 1g are *jointly* described by $\sigma_{LR} \propto \mathbb{1}^{\otimes 2N_v} + Z^{\otimes 2N_v}$, which corresponds to a completely non-local boundary Hamiltonian $H_{LR} = \beta Z^{\otimes 2N_v}$ coupling the two boundaries, with $\beta = \infty$. Imposing a boundary condition on one side (Fig. 1f) leads to $\sigma_{R/L} \propto a\mathbb{1}^{\otimes N_v} + bZ^{\otimes N_v}$, where $a$ and $b$ depend on the corresponding boundary condition, and thus yields an boundary Hamiltonian $H = \beta Z^{\otimes N_v}$, where $\beta$ depends on the boundary conditions, cf. Ref. [9].

To gain a better understanding of the structure of this boundary, it will be helpful to rewrite it as follows: Define $P_{\text{even}} = \frac{1}{2}(\mathbb{1}^{\otimes N_v} + Z^{\otimes N_v})$ and $P_{\text{odd}} = \frac{1}{2}(\mathbb{1}^{\otimes N_v} - Z^{\otimes N_v})$, the projectors onto the even and odd parity subsectors, respectively. Then, we can rewrite $\sigma_{LR} = P_{\text{even}} \otimes P_{\text{even}} + P_{\text{odd}} \otimes P_{\text{odd}}$, i.e., the boundary in Fig. 1g is such that the *total* parity of the left and right boundary is even—the boundary can thus be understood as imposing a parity superselection rule.[1] Correspondingly, by imposing a boundary condition $\chi_R$ on the right side (Fig. 1f), we obtain a boundary state $\sigma_R = p^R_{\text{even}} P_{\text{even}} + p^R_{\text{odd}} P_{\text{odd}}$, with $p^R_{\text{even}} = 1 - p^R_{\text{odd}} = \mathrm{tr}[P_{\text{even}}\chi_R]$. By also fixing a left boundary condition $\chi_L$ (with $p^L_{\text{even}}$ and $p^L_{\text{odd}}$ defined accordingly), we find that the boundary Hamiltonian is $H = -\log p_{\text{even}} P_{\text{even}} - \log p_{\text{odd}} P_{\text{odd}}$ (with $p_{\text{even}} = p^L_{\text{even}} p^R_{\text{even}}$, and $p_{\text{odd}} = p^L_{\text{odd}} p^R_{\text{odd}}$). Thus, the boundary Hamiltonian at the RG fixed point acts by changing the weight of the parity subsectors, with the weight given by the boundary conditions. (Note that the choice of the boundary $\chi$ in the PEPS can be achieved by choosing appropriate boundary terms in the corresponding *physical* Hamiltonian.)

We would now like to go beyond the RG fixed point and study how topological order is reflected in the boundary, and whether there is a way to detect topological phase transitions and the disappeareance of topological order. In order to study these phenomena, we will consider the toric code with string tension which is obtained by introducing a specific magnetic field. This model has been first discussed in [18], where it was shown that it exhibits a topological phase transition by mapping it to the 2D classical Ising model; see also [19]. The ground state of the model has an exact PEPS representation which can be constructed from the tensor of the toric code (cf. Ref. [13], Eq. 7.5) by acting with an invertible map $\Lambda$ which supresses $|1\rangle$ states (strings) by a weight $\lambda \leq 1$. Here, $\lambda = 1$ corresponds to the toric code, and $\lambda = 0$ to the vacuum; the phase transition occurs at $\lambda = 1/\sqrt{1+\sqrt{2}} \approx 0.644$ [18]. (Note that since $\Lambda$ is invertible, we can kick it back to the toric code Hamiltonian to obtain an exact frustration-free Hamiltonian for the deformed model [20]).

The presence of a gauge symmetry, Fig. 1b, in the tensor is the only known way to achieve topological order in PEPS. Let us therefore try to understand what the presence of such a symmetry implies for the structure of the boundary. For now, we will focus on a cylinder of fixed circumference $N_v$, where we will take its length $N_h$ to infinity. By blocking the tensors in a column, we obtain a description of the state on the cylinder as a Matrix Product State (MPS) [21, 22] (i.e., a one-dimensional tensor network), characterized by a tensor $T \equiv T^i_{\alpha\beta}$. $T$ inherits the symmetry from the PEPS tensors, $T^i = \tilde{Z} T^i \tilde{Z}$, with $\tilde{Z} = Z^{\otimes N_v}$, i.e., the matrices $T^i$ are block-diagonal, with the two blocks corresponding to the even and odd parity subsector, respectively. It follows [22] that the transfer operator $\mathbb{T} = \sum T^i \otimes \bar{T}^i$, Fig. 1e, has positive maximal left (right) eigenvectors in both sectors, $\sigma^L_{\mathrm{even}}$ ($\sigma^R_{\mathrm{even}}$) and $\sigma^L_{\mathrm{odd}}$ ($\sigma^R_{\mathrm{odd}}$), with corresponding eigenvalues $\gamma_e$ and $\gamma_o$. Using the Cauchy-Schwarz inequality, it is straightforward to see that the largest eigenvalue $|\gamma_{eo}|$ of the off-diagonal block is bounded as $|\gamma_{eo}| < \sqrt{\gamma_e \gamma_o}$: This is, for a sufficiently long cylinder the boundary states $\sigma_L$ and $\sigma_R$, and thus $\sigma \propto \sqrt{\sigma_L^*}\sigma_R\sqrt{\sigma_L^*}$, will be block-diagonal (up to an exponentially small correction) for any boundary condition, $\sigma = p_{\mathrm{even}}\sigma_{\mathrm{even}} \oplus p_{\mathrm{odd}}\sigma_{\mathrm{odd}}$. (Here, $\sigma_{\mathrm{even}} \propto \sqrt{\sigma^{L*}_{\mathrm{even}}}\sigma^R_{\mathrm{even}}\sqrt{\sigma^{L*}_{\mathrm{even}}}$, $\sigma_{\mathrm{odd}} \propto \sqrt{\sigma^{L*}_{\mathrm{odd}}}\sigma^R_{\mathrm{odd}}\sqrt{\sigma^{L*}_{\mathrm{odd}}}$, and $\mathrm{tr}\,\sigma_{\mathrm{even}} = \mathrm{tr}\,\sigma_{\mathrm{odd}} = 1$.) Again, $p_{\mathrm{even}}$ and $p_{\mathrm{odd}}$ depend on the boundary conditions $\chi$. Conversely, for a given $N_h$ we can always choose boundary conditions $\chi$ such that any such $\sigma$ is realized.

---

[1] This parity can be understood as arising from fermions with internal degrees of freedom: E.g., the toric code has $Z = \left(\begin{smallmatrix}1 & \\ & -1\end{smallmatrix}\right)$, i.e., spinless fermions [13], and the RVB state has $Z = \mathrm{diag}(1, 1, -1)$, i.e., spinful fermions with a hardcore constraint such as in the $t$-$J$-model [16, 17].

As we have seen, the virtual boundary of a system with topological gauge symmetries has a block-diagonal structure $\sigma = p_{\mathrm{even}}\sigma_{\mathrm{even}} \oplus p_{\mathrm{odd}}\sigma_{\mathrm{odd}}$, depending on the parity of the boundary conditions $\chi$. How should we constuct a boundary Hamiltonian from this? A first idea is to choose a boundary condition with fixed parity (w.l.o.g. even), so that $\sigma \propto \sigma_{\mathrm{even}}$, and write $\sigma_{\mathrm{even}} \propto \exp[-H]$. Since $\sigma_{\mathrm{even}}$ is only supported on the even parity sector, $H$ must then be of the form $H = \beta_{\mathrm{topo}} P_{\mathrm{odd}} + H'$, with $\beta_{\mathrm{topo}} = \infty$ and $H' = -\log\sigma_{\mathrm{even}}$ (with the log taken on the even parity subspace). Unfortunately, numerical study quickly reveals that the $H'$ defined this way is highly non-local both in the topological and the non-topological phase (see inset of Fig. 2); in particular, it has strong $N_v - 1$ and $N_v$–body terms. It is in fact easy to see where this comes from: Since $H' = H'Z^{\otimes N_v}$, any local term $h$ in $H'$ comes with a "twin" $hZ^{\otimes N_v}$ which is necessarily highly non-local! There is an *ad hoc* solution to that by noting that $H'$ is not uniquely defined, but only its even parity projection $P_{\mathrm{even}}H'P_{\mathrm{even}} \equiv -\log\sigma_{\mathrm{even}}$. Thus, we can declare the most local $H'$ among all possible choices the "right" one (this corresponds to counting each pair of interactions $h$ and $hZ^{\otimes N_v}$ with the locality of $h$). This solution does indeed show the desired behavior: It gives a local Hamiltonian $H'$ in the topological regime which becomes non-local at the phase transition.

Yet, this *ad hoc* definition of $H'$ might feel unsatisfactory. Fortunately, there is a more elegant solution. To this end, recall that for arbitrary boundary conditions, the boundary state is given by $\sigma = p_{\mathrm{even}}\sigma_{\mathrm{even}} + p_{\mathrm{odd}}\sigma_{\mathrm{odd}}$. If we now consider $H = -\log\sigma$, it follows that it is of the form

$$H = H_{\mathrm{topo}} + H' \ , \tag{1}$$

with

$$H_{\mathrm{topo}} = -\log p_{\mathrm{even}}\,P_{\mathrm{even}} - \log p_{\mathrm{odd}}\,P_{\mathrm{odd}} \tag{2}$$

and

$$H' = -\log\begin{pmatrix}\sigma_{\mathrm{even}} & \\ & \sigma_{\mathrm{odd}}\end{pmatrix} \ . \tag{3}$$

We thus find that the Hamiltonian splits into two parts: The first part, $H_{\mathrm{topo}}$, depends on the choice of boundaries $\chi$, and it controls the relative weight of the even and odd parity subspace and is therefore nonlocal—in fact, it is exactly the same as the one we found for the toric code earlier. The second part, $H'$, on the other hand, is independent of the boundary conditions $\chi$; it only depends on the fixed points of the transfer operators in each parity sector and is thus uniquely defined. Since $H_{\mathrm{topo}} = 0$ for $p_{\mathrm{even}} = p_{\mathrm{odd}}$, $H' = H$ equals the actual entanglement Hamiltonian for appropriate boundary conditions; moreover, any boundary condition with $p_{\mathrm{even}} \neq p_{\mathrm{odd}}$ will generally result in a less local $H$ since $H_{\mathrm{topo}} \propto Z^{\otimes N_v} + \mathrm{const}$. The numerical results for the locality of $H'$ for the toric code with string tension are shown in Fig. 2: We find that $H'$ is short-ranged in the topologically ordered regime, becomes long-ranged at the phase transition, and remains so in the entire non-topological regime. We have then used this finding to study the interpolation between the square lattice Toric Code and the RVB state on the kagome lattice described in [16]. The result is shown in Fig. 3: The boundary Hamiltonian $H'$ is local throughout, and no sign of a phase transition can be found, thus strongly supporting the existing evidence that the RVB state is a topological

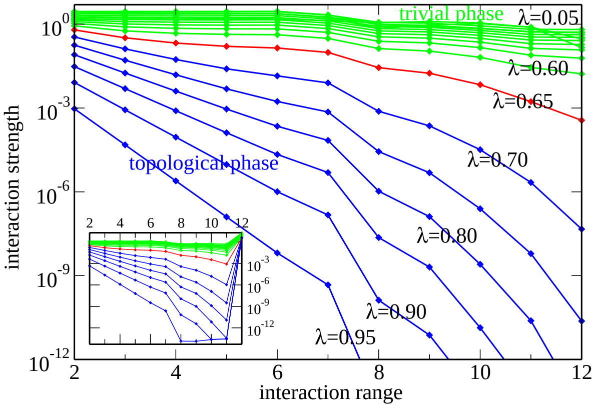

FIG. 2. Interaction range of the boundary Hamiltonian (3) for the toric code with magnetic field, for $N_v = 12$. $\lambda = 1$ is the toric code, $\lambda = 0$ the trivial state, and $\lambda \approx 0.644$ the phase transition (red). Blue (green) denote the topological (trivial) phase. The interaction range of the boundary Hamiltonian (as defined in Ref. [9]) decays exponentially in the topological phase, while it is long-ranged in the trivial phase. (To exclude finite-size effects, only points up to $N_v/2 = 6$ should be considered for the decay.) The inset shows the Hamiltonian defined only from $\sigma_{\mathrm{even}}$, which has strong 12-body terms in both phases. The calculations (as well as the ones in Figs. 3 and 4) have been carried out using exact column-wise contraction (cf. [9, 16, 17]) and are thus exact.

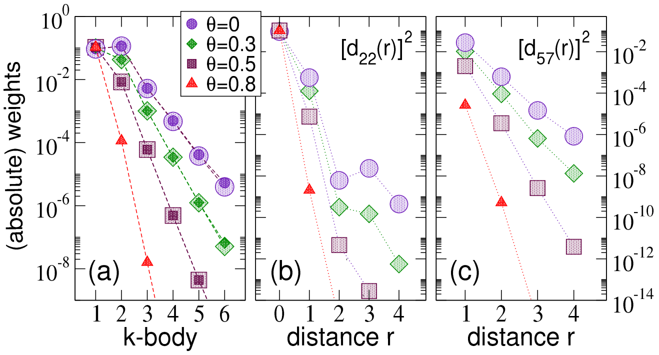

FIG. 3. Interaction range for the Toric Code–kagome RVB interpolation [16] for $N_v = 8$ (large symbols) and $N_v = 6$ (small symbols). (a) shows the strength of $k$-body terms, while (b) and (c) analyze the decay of two specific two-body terms (see Ref. [17]) with distance. It is found that all terms decay exponentially throughout the interpolation, showing the absence of a topological phase transition between the toric code and the RVB system.

$\mathbb{Z}_2$ spin liquid.

The decomposition (1) of the entanglement Hamiltonian into $H_{\rm topo}$ and $H'$ can be understood as follows: $H_{\rm topo}$ consitutes the *universal* part of the boundary Hamiltonian—it controls the relative weight of the parity sectors and is therefore completely non-local, does not depend on the microscopic details of the phase (here, $\lambda$), is invariant under renormalization, and captures long-range features such as the fact that the two boundaries are connected. $H'$, on the other hand, is *non-universal*—it depends on the microscopic details of the phase, and it vanishes under renormalization in the topological phase; on the other hand, it becomes long-ranged at the phase transition and thus destroys the topological order otherwise contained in $H_{\rm topo}$.

What happens if we consider a PEPS cylinder with two virtual boundaries, Fig. 1g, which is what we e.g. encounter if we want to study the ES on a torus? If $\sigma_L = \sigma_R^*$, we have that $\mathbb{T}^\infty = \sigma_{\rm even}\otimes\sigma_{\rm even} + \sigma_{\rm odd}\otimes\sigma_{\rm odd}$, which implies that the boundary Hamiltonian is of the form

$$H = \beta_{\rm topo}(P_{\rm even}\otimes P_{\rm even} + P_{\rm odd}\otimes P_{\rm odd}) + H'\otimes \mathbb{1} + \mathbb{1}\otimes H' \ ,$$

where $\beta_{\rm topo}=\infty$, and $H'$ again as in Eq. (3): The universal topological part couples the two boundaries and imposes that they joinly have even parity, while the non-universal part is the same local Hamiltonian as before, acting independently on both boundaries. ( If $\sigma_L^*\neq\sigma_R$, $H'$ is different on the left and on the right.)

The form (1) of the boundary Hamiltonian has also consequences for the topological entropy $S(\rho_L) = S(\sigma)$: We have that

$$S(\rho_L) = H(p_{\rm even}) + p_{\rm even}S(\sigma_{\rm even}) + p_{\rm odd}S(\sigma_{\rm odd}) \ , \quad (4)$$

where $H(p) = -p\log p - (1-p)\log(1-p)$, i.e., depending on the choice of the boundary condition, the topological correction can be maximal ($p_{\rm even}=1$ or $p_{\rm odd}=1$), zero ($p_{\rm even}=p_{\rm odd}=\frac{1}{2}$) or anywhere inbetween.

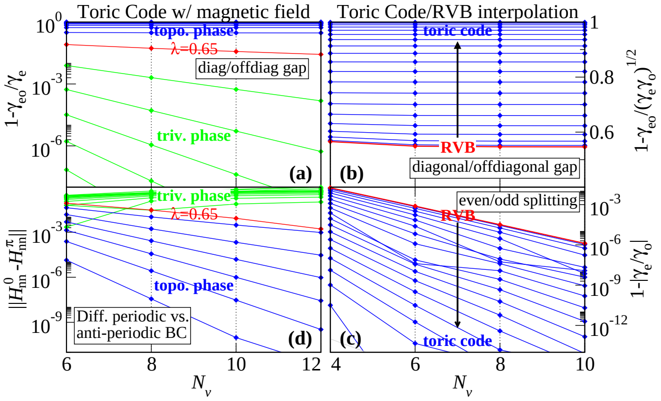

FIG. 4. Scaling analysis (cf. text). (a) Diagonal/offdiagonal gap for the toric code with string tension. (b) Same for the interpolation between square lattice toric code and the RVB state on the kagome lattice [16]. (c) Splitting between even and odd block for the Toric Code–RVB interpolation. (d) Different of the phase-corrected nearest-neighbor terms for the two boundary Hamiltonians $H^0$ and $H^\pi$. In all cases, the interpolation parameter $0\le\lambda\le1$ is increased in steps of 0.05. $\gamma_e$, $\gamma_o$, and $\gamma_{eo}$ are the largest eigenvalue of the even, odd, and off-diagonal block of the transfer operator, respectively.

Up to now, we have considered systems in the limit where $N_h\to\infty$ for finite $N_v$; we exploited this in particular when deriving the block-diagonal structure of the boundary. Does this limit correctly reproduce the physics of systems where we take the simultaneous limit in $N_h$ and $N_v$? In order to understand this, we need to study the properties of the transfer operator as a function of $N_v$.

Firstly, in order to obtain a block-diagonal boundary operator, it is important that the off-diagonal blocks are supressed relative to the diagonal ones for $N_v\to\infty$. Fig. 4a shows this data for the toric code with string tension: In the topological phase (blue), the supression converges to a constant as required; in the trivial phase (green), on the other hand, the supression vanishes exponentially in $N_v$, and our limit is no longer justified. Fig. 4b shows the same data for the toric code–RVB interpolation, proving that the off-diagonal blocks are indeed supressed throughout.

Secondly, if the eigenvalues corresponding to the even and odd parity subsector are not equal, in principle only one of them contributes to the boundary state for $N_h\to\infty$. For the Toric Code with string tension, there is no such splitting due to symmetries; for the Toric Code – RVB interpolation, Fig. 4c proves that this splitting vanishes exponentially in $N_v$. (Note though that even with a finite splitting, all topological sectors will appear as ground states in the thermodynamic limit as they are not coupled by the Hamiltonian [23]).

Up to now, we have only considered one of the two ground states on the cylinder which exist for a fixed boundary condition. The second ground state can be obtained by moving one excitation from one boundary to the other; in the PEPS representation, this is achieved by placing a string of $Z$'s connecting the boundaries on the bonds [13]. This already suggests that the difference between the boundary Hamiltonians lies in the presence of a $\pi$ flux through the torus, which gives rise to a Berry phase: We expect that the boundary Hamiltonian $H^{\pi}$ with $Z$ string is the same as the one without, $H^{0}$, except for a phase $e^{i\pi}$ for any term which describes hopping across the location of the $Z$ string. Fig. 4d shows the difference between the nearest neighbor terms in $H^{0}$ and $H^{\pi}$ after undoing the $e^{i\pi}$ phase in $H^{\pi}$, which indeed vanishes exponentially with $N_v$ in the topological phase; the same behavior is observed for longer-range terms. Taking superpositions of these two ground states can be understood as entangling the flux $|\phi\rangle$ with $H^{\phi}$; this increases (4) (and thus decreases the topological correction) by the mixing entropy.

To conclude, we have studied the boundary Hamiltonian of topologically ordered models and found that it consists of two parts: A non-local universal part which encodes the topological features of the system, and a local non-universal part which depends on the details of the system within the topological phase. The topological order is destroyed when the non-universal part looses its locality. The structure of the universal part is given by the symmetry underlying the model, which can be interpreted in terms of particles with conservation laws which are given by the topological model under consideration (such as a group for double models, of a general fusion rule for string nets). It is an extremely suggestive idea that such a decomposition should exist for any phase, i.e., that for any phase there exists a universal contribution of the boundary Hamiltonian such that the remaining non-universal part becomes local, and this very universal part would then label the phase of the sytem.

*Acknowledgements.*—We acknowledge helpful discussions with F. Verstraete. NS acknowledges support by the Alexander von Humboldt foundation, the Caltech Institute for Quantum Information and Matter (an NSF Physics Frontiers Center with support of the Gordon and Betty Moore Foundation) and the NSF Grant No. PHY-0803371. DP acknowledges support by the Agence Nationale de la Recherche under grant No. ANR 2010 BLANC 0406-0, and CALMIP (Toulouse) for supercomputer ressources. JIC acknowledges support by the EU project AQUTE, the DFG SFB 631 and Exzellenzcluster NIM, and Catalunya Caixa. DP-G acknowledges QUEVADIS and Spanish grants QUITEMAD and MTM2011-26912.

---

[1] A. Kitaev and J. Preskill, Phys. Rev. Lett. **96**, 110404 (2006), hep-th/0510092.

[2] M. Levin and X.-G. Wen, Phys. Rev. Lett. **96**, 110405 (2006), cond-mat/0510613.

[3] H. Li and F. D. M. Haldane, Phys. Rev. Lett. **101**, 010504 (2008), arXiv:0805.0332.

[4] D. Poilblanc, Phys. Rev. Lett. **105**, 077202 (2010), arXiv:1005.2123.

[5] A. M. Läuchli and J. Schliemann, Phys. Rev. B **85**, 054403 (2012), arXiv:1106.3419.

[6] J. Schliemann, Phys. Rev. B **83**, 115322 (2011), arXiv:1008.5289.

[7] L. Fidkowski, (2009), arXiv:0909.2654.

[8] X.-L. Qi, H. Katsura, and A. W. W. Ludwig, Phys. Rev. Lett. **108** (2012), arXiv:1103.5437.

[9] J. I. Cirac, D. Poilblanc, N. Schuch, and F. Verstraete, Phys. Rev. B **83**, 245134 (2011), arXiv:1103.3427.

[10] F. Verstraete and J. I. Cirac, (2004), cond-mat/0407066.

[11] M. B. Hastings, Phys. Rev. B **76**, 035114 (2007), cond-mat/0701055.

[12] A. Kitaev, Ann. Phys. **303**, 2 (2003), quant-ph/9707021.

[13] N. Schuch, I. Cirac, and D. Pérez-García, Ann. Phys. **325**, 2153 (2010), arXiv:1001.3807.

[14] O. Buerschaper, J. M. Mombelli, M. Christandl, and M. Aguado, (2010), arXiv:1007.5283.

[15] M. A. Levin and X.-G. Wen, Phys. Rev. B **71**, 045110 (2005), cond-mat/0404617.

[16] N. Schuch, D. Poilblanc, J. I. Cirac, and D. Pérez-García, Phys. Rev. B **86**, 115108 (2012), arXiv:1203.4816.

[17] D. Poilblanc, N. Schuch, D. Pérez-García, and J. I. Cirac, Phys. Rev. B **86**, 014404 (2012), arXiv:1202.0947.

[18] C. Castelnovo and C. Chamon, Phys. Rev. B **77**, 054433 (2008), arXiv:0707.2084.

[19] S. Trebst, P. Werner, M. Troyer, K. Shtengel, and C. Nayak, Phys. Rev. Lett. **98**, 070602 (2007), cond-mat/0609048.

[20] N. Schuch, D. Perez-Garcia, and I. Cirac, Phys. Rev. B **84**, 165139 (2011), arXiv:1010.3732.

[21] M. Fannes, B. Nachtergaele, and R. F. Werner, Commun. Math. Phys. **144**, 443 (1992).

[22] D. Perez-Garcia, F. Verstraete, M. M. Wolf, and J. I. Cirac, Quant. Inf. Comput. **7**, 401 (2007), quant-ph/0608197.

[23] L. Cincio and G. Vidal, (2012), arXiv:1208.2623.